Frequency Response of Cross-Phase Modulation in Multispan WDM Optical Fiber Systems

R. Hui, *Senior Member, IEEE,* Y. Wang, K. Demarest, *Member, IEEE,* and C. Allen, *Senior Member, IEEE*

***Abstract*— The spectral characteristics of cross-phase modulation (XPM) in multispan intensity-modulation direct-detection optical systems were investigated both experimentally and theoretically. XPM crosstalk levels and its spectral features were found to be strongly dependent on fiber dispersion and optical signal channel spacing. Interference between XPM-induced crosstalk effects created in different amplified fiber spans is also found to be important to determine the overall frequency response of XPM crosstalk effects.**

***Index Terms*— Crosstalk, optical fiber communication, optical fiber nonlinearity, WDM optical systems.**

I. Introduction

CROSS-PHASE modulation (XPM) has been found to have an important impact in the performance of high-speed wavelength-division-multiplexed (WDM) optical fiber communication systems [1], [2]. Due to the Kerr effect in optical fibers, intensity modulation of one optical carrier can modulate the phases of other copropagating optical signals in the same fiber. Unlike coherent optical systems, intensity-modulation direct-detection (IMDD) optical systems are not particularly sensitive to signal phase fluctuations. Therefore, the crosstalk-induced phase modulation is not a direct source of IMDD systems performance degradation. However, due to chromatic dispersion of optical fibers, phase modulation can be converted into intensity modulation [3] and, thus, can degrade the IMDD system performance.

It has been found that XPM created phase modulation is inversely proportional to the baseband signal modulation frequency [4]. On the other hand, since the phase-to-intensity conversion through fiber dispersion is also a function of the modulation frequency [3], the overall intensity-to-intensity crosstalk will be a combination of these two effects. Since XPM is an important source of performance degradation in dense WDM optical systems, a better understanding of XPM-induced crosstalk and its frequency response is indispensable in the systems design and their performance evaluation.

In this letter, we report the results of our measurements on the XPM frequency response of a multispan WDM optical system. The crosstalk level is found to be dependent on the optical channel spacing and fiber dispersion. Interference between XPM-induced crosstalk effects created in different amplified optical spans is also found to be important to determine the overall spectrum features of XPM-induced crosstalk. A simple analytical expression is obtained to describe the XPM-induced crosstalk. Excellent agreement between measurements and theoretical predictions has been obtained.

The theoretical analysis begins with the nonlinear wave propagation equation [5]. Consider probe and pump optical signals, $A_j(t, z)$ and $A_k(t, z)$, copropagating in the same optical fiber:

$$\frac{\partial A_j(t,z)}{\partial z} + \frac{\alpha}{2}A_j(t,z) + \frac{1}{v_j}\frac{\partial A_j(t,z)}{\partial t} + \frac{i\beta_2}{2}\frac{\partial^2 A_j(t,z)}{\partial^2 t} = i\gamma_j[p_j(t,z) + 2p_k(t - d_{jk}z, z)]A_j(t,z) \quad (1)$$

where α is the attenuation coefficient of the fiber, $\gamma_j = 2\pi n_2/(\lambda_j A_{\text{eff}})$ is the nonlinear coupling coefficient, n_2 is the nonlinear refractive index, λ_j and λ_k are the probe and the pump signal wavelengths, A_{eff} is the fiber effective core area, $p_k = |A_k|^2$ and $p_j = |A_j|^2$ are optical powers of the pump and the probe signals, $d_{jk} \equiv (1/v_j) - (1/v_k)$ is the relative walkoff between the two signals with $v_{j,k}$, the group velocities of the two channels. Through linear approximation, the walkoff can be expressed as $d_{jk} = S_0(\lambda - \lambda_0)\Delta\lambda_{jk}$, where λ_0 and S_0 are fiber zero-dispersion wavelength and dispersion slope and $\Delta\lambda_{jk}$ is the wavelength spacing between the probe and the pump signals.

In order to simplify the analysis and to be able to focus our attention on the effect of interchannel crosstalk, we suppose that the probe signal is operated in continuous-wave (CW) whereas the pump signal is modulated with a sinusoid wave at the frequency ω. Under this condition and with small signal approximation, the probe signal self-phase modulation (SPM) can be neglected and thus the first term on the right-hand side (RHS) of (1) can be removed. Translating this propagation equation into the frequency domain using Fourier transformation, we have

$$\frac{\partial \tilde{A}_j(\Omega,z)}{\partial z} = \left\{-\left(\frac{\alpha}{2} + \frac{i\Omega}{v_j}\right) + i\gamma_j 2p_k(\Omega,0) \cdot e^{i\Omega d_{jk}z}e^{-\alpha z} + \frac{i\beta_2\Omega^2}{2}\right\}\tilde{A}_j(\Omega,z) \quad (2)$$

where $\tilde{A}(\Omega, z)$ is the Fourier transformation of $A(t, z)$ and $p_k(\Omega, 0)$ is the power spectrum of the pump signal at the system input. On the RHS of (2), the first term accounts for attenuation and linear phase delay. The second term is responsible for phase modulation in the probe signal (j)

Manuscript received February 17, 1998; revised May 15, 1998. This work was supported in part by the Sprint Corporation and by the National Science Foundation under Grant EPSCoR/ECS 963-2617.

The authors are with the Information and Telecommunication Technology Center, Department of Electrical Engineering and Computer Science, The University of Kansas, Lawrence, KS 66045 USA.

Publisher Item Identifier S 1041-1135(98)06274-0.

induced by the pump signal (k). This phase modulation is proportional to the optical power in the pump signal and the fiber nonlinearity. In a short fiber section dz, the crosstalk phase modulation in the probe signal, induced by the pump signal, can be linearized under the small signal approximation [4]

$$d\phi_{jk}(\Omega, z) = 2\gamma_j p_k(\Omega, 0)e^{(-\alpha + i\Omega\, d_{jk})z}\, dz. \tag{3}$$

Now, look at the third term on the RHS of (2). This is the term responsible for the phase noise to intensity noise conversion in the probe signal. Phase noise generated at $z = z'$ is converted into intensity noise at the end of the fiber $z = L$ due to chromatic dispersion. As discussed in [3], the in-phase component of this conversion is proportional to $\sin[\beta_2\Omega^2(L-z)/2]$. Integrating all XPM contributions along the fiber, adding fiber loss and linear phase delay, we can obtain the total intensity noise at the end of the fiber $z = L$

$$\begin{aligned}\Delta\tilde{A}_j(\Omega, L) = \sqrt{p_j(L)}e^{-i\Omega/v_j L}\int_0^L 2\gamma_j p_k(\Omega, 0)\\ \cdot e^{-(\alpha - i\Omega\, d_{jk})z}\sin[\beta_2\Omega^2(L-z)/2]\, dz\end{aligned} \tag{4}$$

where $p_j(L)$ is the probe signal average optical power at the end of the fiber $z = L$. Under the assumptions that $\exp(-\alpha L) \ll 1$ and the modulation bandwidth is much smaller than the channel spacing, i.e., $d_{jk} \gg \beta_2\Omega/2$, we can find a simple form to describe the relative amplitude fluctuation induced by XPM as

$$\begin{aligned}\Delta a_{jk}(\Omega, L) &= \frac{\Delta\tilde{A}_j(\Omega, L)}{\sqrt{p_j(L)}}\\ &= \gamma_j p_k(\Omega, 0)\frac{\sin(\beta_2\Omega^2 L/2)}{\alpha - i\Omega d_{jk}}\, e^{-i\Omega/v_j L}\end{aligned} \tag{5}$$

where $a_{jk}(\Omega, L)$ is the XPM-induced amplitude modulation in the probe signal, normalized to the field amplitude in this channel without crosstalk. In multispan, optically amplified systems, the total amplitude fluctuation at the receiver is the sum of XPM contributions created by each fiber span. Under the assumption that the length of each span is much longer than the fiber nonlinear length [1], which is typically about 20 km, the normalized XPM frequency response can be expressed as

$$\begin{aligned}\Delta p_{jk}(\Omega, L_N) = \Bigg|\sum_{i=1}^{N}\Bigg\{\gamma_j p_k^{(i)}(\Omega, 0)\exp[-i\Omega\, d_{jk}^{(i-1)}L^{(i-1)}]\\ \cdot\frac{\sin\left[\Omega^2\sum_{n=i}^{N}\beta_2^{(n)}L^{(n)}/2\right]}{\alpha - i\Omega d_{jk}^{(i)}}\Bigg\}\Bigg|^2\end{aligned} \tag{6}$$

where $L_N = \sum_{n=1}^{N} L^{(n)}$ is the total fiber length in the system with N spans, N is the number of spans, $L^{(i)}$ and $\beta^{(i)}$ are fiber length and dispersion of the ith span with $L^{(0)} = 0$, $p_k^{(i)}(\Omega, 0)$ is the pump signal input power spectrum of the ith span and $d_{jk}^{(i)}$ is the relative walkoff between two channels in the ith span, where $d_{jk}^{(0)} = 0$. Equation (6) describes the XPM-induced intensity modulation in the probe signal, normalized to its power level without this effect.

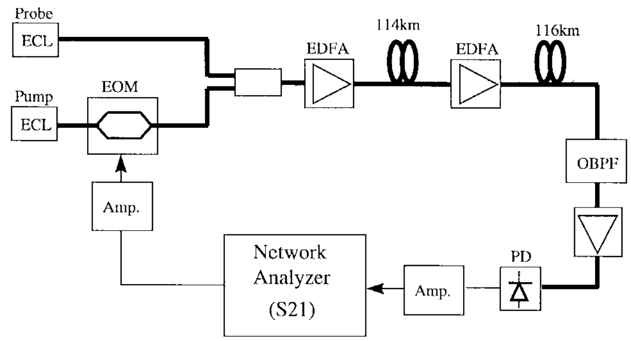

Fig. 1. Experimental setup. ECL: external cavity semiconductor laser. OBPF: optical bandpass filter. Amp.: microwave amplifier. EOM: external optical modulator. PD: photodiode.

Our experimental setup, designed to measure the XPM frequency response, is shown in Fig. 1. Two external-cavity tunable semiconductor lasers (ECL) emitting at λ_j and λ_k are used as sources for the probe and the pump signals, respectively. The probe signal operates as CW and the pump signal is externally modulated by the signal coming from a microwave network analyzer. The two optical signals are combined through a 3-dB coupler and then sent to an optical amplifier to boost the optical power. The optical system in the experiment has two nonzero dispersion shifted fiber spans with lengths of 114 and 116 km, respectively. A tunable optical filter is used at the receiver to select the probe signal and suppress the pump signal. After passing through an optical preamplifier, the signal is detected by a 32-GHz bandwidth photodiode, amplified by a 10-GHz bandwidth microwave amplifier, and then sent to the receiver port of the network analyzer. The optical power injected into each fiber span is fixed at approximately 11.5 dBm at each channel. Due to XPM-induced crosstalk, the probe signal output, which was initially CW, is intensity modulated by the pump signal.

Fig. 2 shows the normalized XPM frequency response measured at the output of the system with only a single 114 km fiber span. The channel spacings used to obtain this figure were 0.8 nm ($\lambda_j = 1559$ nm, $\lambda_k = 1559.8$ nm) (stars) and 1.6 nm ($\lambda_j = 1559$ nm, $\lambda_k = 1560.6$ nm) (circles). Continuous lines are calculated using (6). Parameters used in the calculation are: $\lambda_0 = 1520.2$ nm, $S_0 = 0.075$ ps/km/nm^2, $n_2 = 2.35 \cdot 10^{-20}$ m$^2 \cdot$ /W, $A_{\rm eff} = 5.5 \cdot 10^{-11}$ m^2, $\alpha = 0.25$ dB/km and the pump signal input optical power $p_k(z=0) =$ 11.5 dBm with its modulation frequency swept from 50 MHz to 10 GHz. High-pass characteristics are clearly demonstrated in both curves in Fig. 2 and XPM crosstalk levels are higher with narrower channel spacing. This is qualitatively different from the results obtained in [4] where only phase modulation index was concerned, which is inversely proportional to the signal baseband modulation frequency. However, since the efficiency of phase to intensity modulation conversion through the fiber dispersion is proportional to $\sin(\beta_2\Omega^2 L/2)$, as indicated in (4), the crosstalk in the low frequency part is

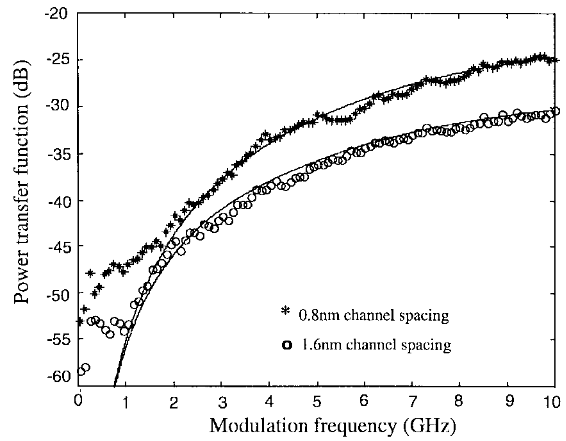

Fig. 2. XPM frequency response in the system with single span (114 km) nonzero dispersion shifted fiber. Stars: 0.8-nm channel spacing ($\lambda_{\mathrm{probe}} =$ 1559 nm and $\lambda_{\mathrm{pump}} = 1559.8$ nm). Open circles: 1.6-nm channel spacing ($\lambda_{\mathrm{probe}} = 1559$ nm and $\lambda_{\mathrm{pump}} = 1560.6$ nm). Continuous lines are corresponding theoretical results.

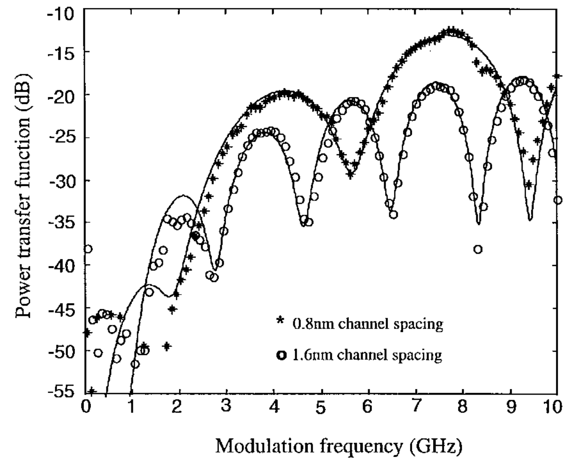

Fig. 3. XPM frequency response in the system with two spans (114 and 116 km) of nonzero dispersion shifted fiber. Stars: 0.8-nm channel spacing ($\lambda_{\mathrm{probe}} = 1559$ nm and $\lambda_{\mathrm{pump}} = 1559.8$ nm). Open circles: 1.6-nm channel spacing ($\lambda_{\mathrm{probe}} = 1559$ nm and $\lambda_{\mathrm{pump}} = 1560.6$ nm). Continuous lines are corresponding theoretical results.

greatly suppressed and this brings the overall XPM frequency response to a high-pass like characteristic. We believe that the discrepancy between theoretical and experimental results in the low frequency part is caused by the frequency discrimination effect introduced through the narrow-band optical filter.

Fig. 3 shows the XPM frequency response measured in the system with two optical fiber spans, as shown in Fig. 1, with 0.8-nm (stars) and 1.6-nm (open circles) optical channel spaces. Corresponding theoretical results calculated from (6) are also displayed. It is very interesting to note that in the system with many optical spans, the ripple of XPM frequency response is strongly dependent on the channel spacing. This is because of the interference between XPM-induced crosstalks created in the different fiber spans. From (6), it is easy to see that the frequency difference between adjacent notches of a spectrum is $\Delta f = 1/(d_{jk}L_1)$ with L_1 the fiber length of the first span.

In conclusion, spectral characteristics of XPM in multispan WDM systems have been evaluated both experimentally and theoretically. The crosstalk level is found to be dependent on optical channel spacing and fiber dispersion. Interference between XPM crosstalks created in different fiber spans creates strong ripples in the frequency response. A simple analytical expression was obtained to describe the XPM-induced crosstalk. An excellent agreement between measurements and theoretical prediction has been obtained.

REFERENCES

[1] A. R. Chraplyvy, “Limitations of lightwave communications imposed by optical fiber nonlinearities,” *J. Lightwave Technol.*, vol. 8, pp. 1548–1557, Oct. 1990.

[2] D. Marcus, A. R. Chraplyvy, and R. W. Tkach, “Dependence of cross-phase modulation on channel number in fiber WDM systems,” *J. Lightwave Technol.*, vol. 12, pp. 885–890, May 1994.

[3] J. Wang and K. Petermann, “Small signal analysis for dispersive optical fiber communication systems,” *J. Lightwave Technol.*, vol. 10, pp. 96–100, Jan. 1992.

[4] T.-K. Chiang, N. Kagi, M. E. Marhic, and L. Kazovsky, “Cross-phase modulation in fiber links with multiple optical amplifiers and dispersion compensators,” *J. Lightwave Technol.*, vol. 14, pp. 249–260, Mar. 1996.

[5] G. P. Agrawal, *Nonlinear Fiber Optics*. San Diego, CA: Academic, 1989.